Journal of Fluids and Structures (1999) **13,** 663–680
Article No.: jfls. 1999.0230 available online at http://www.idealibrary.com on IDEAL

ABSOLUTE AND CONVECTIVE BENDING INSTABILITIES IN FLUID-CONVEYING PIPES

E. DE LANGRE
Laboratoire d'Hydrodynamique, CNRS, École Polytechnique
91128 Palaiseau, France
and
Département de Mécanique et Technologie, Commissariat à l'Energie Atomique
Saclay, 91191 Gif-sur-Yvette, France

AND

A. E. OUVRARD
Laboratoire d'Hydrodynamique, CNRS, École Polytechnique
91128 Palaiseau, France

(Received 9 December 1998 and in revised form 27 May 1999)

The effect of internal plug flow on the lateral stability of fluid conveying pipes is investigated by determining the absolute or convective nature of the instability from the analytically derived linear dispersion relation. The fluid–structure interaction is modelled by following the work of Gregory & Païdoussis. The formulation of the fluid-conveying pipe problem is shown to be related to previous studies of a flat plate in the presence of uniform flow by Brazier-Smith & Scott and Crigthon & Oswell. The different domains of stability, convective instability, and absolute instability are explicitly derived in control parameter space. The effects of flow velocity, fluid–structure mass ratio, stiffness of the elastic foundation, bending rigidity and axial tension are considered. Absolute instability in flexural pipes prevails over a wide range of parameters. Convective instability is mostly found in tensioned pipes, which are modelled by a generalized linear Klein–Gordon equation. The impulse response is given in closed form or as an integral approximation and its behaviour confirms the results found directly from the dispersion equation.

1. INTRODUCTION

INTERACTIONS BETWEEN A MOVING FLUID and an elastic boundary give rise to a large variety of physical phenomena that need to be understood from both a fundamental and applied point of view. Flow stability is known to be modified by the compliance of an adjacent solid boundary, which might have some influence on the magnitude of drag. Conversely, the stability of the solid boundary may be affected by the flow, thereby leading to unacceptable mechanical strains. According to the fundamental analyses of Landahl (1962) and Benjamin (1963), energy exchanges between the solid and the fluid media may give rise to a profusion of instability types even in deceptively simple physical models.

Instabilities that develop both in space and time may be classified as convective or absolute, according to the nature of the long-time impulse response. This theoretical framework, now of common use in hydrodynamics (Huerre & Monkewitz 1990), has also been fruitfully applied to fluid–structure interactions problems. The generic case of inviscid

0889–9746/99/060663 + 18 $30.00

uniform flow above an elastic plate, further referred to as the flat-plate problem, has been extensively analysed (Brazier-Smith & Scott 1984; Carpenter & Garrad 1986; Crighton & Oswell 1991; Lucey & Carpenter 1992; Peake 1997) and extended to membranes under tension (Kelbert & Sazonov 1996). These analyses have brought to light many of the fundamental features of these interactions, such as the existence of negative energy waves or possible violations of the usual out-going wave radiation condition.

In the vast domain of fluid–structure interactions, the specific problem of bending vibrations of fluid-conveying pipes has drawn the attention of a large community, because of the fascinating variety of dynamical properties that are exhibited by these simple systems (Païdoussis & Li 1993). In a pioneering work, Bourrières (1939) derived the equation of motion of a beam-like structure that conveys fluid and examined the stability of finite length pipes. This problem was subsequently solved by Gregory & Païdoussis (1966) for the particular case of a cantilevered pipe which displays the well-known garden-hose instability. Since then, finite-length systems have been extensively studied, under all possible varieties of flow conditions or mechanical characteristics (Païdoussis & Li 1993).

Comparatively little attention has been paid to the question of wave propagation in such systems. The stability conditions for harmonic waves were derived by Roth (1964), who clearly identified for all wavepackets a common convection velocity that is smaller than the fluid velocity. Stein & Tobriner (1970), by the use of numerical simulations, could display the evolution of stable wavepackets with time. More recently, Kulikovskii & Shikina (1988) found that the mass ratio between the fluid and the pipe had a crucial effect on the convective or absolute nature of the instability. A slender cylindrical structure exposed to external axial flow may be modelled by equations identical in form to those of the fluid-conveying pipe (Païdoussis 1987). For that geometry, Triantafyllou (1992) succeeded in exhibiting the physical nature of the various families of waves that come into play by analysing the origin of their energy density.

The goal of the present paper is to systematically determine the convective or absolute nature of instabilities that may arise in an infinite pipe conveying fluid, as a function of several physical parameters such as the flexural rigidity, the tension, the foundation stiffness, or the flow velocity, thereby extending the work of Kulikovskii & Shikina (1988) and Triantafyllou (1992). The impulse response is also sought in explicit form to confirm and illustrate results derived from the analysis of the dispersion relation. The variety of possible transitions is underscored by considering the general case as well as the extreme values of the nondimensional parameters. We finally demonstrate the relationship between such models of fluid-conveying pipes and those involving semi-infinite flow over an elastic plate or membrane. The long-range objective is to identify the local nature of the instabilities in order to ultimately shed some light on the global dynamics of fluid-conveying systems of finite length.

Let us recall the dynamical equation governing small lateral motions of an initially straight fluid-conveying pipe, as sketched in Figure 1. Under the plug-flow assumption, the fluid motion may be explicitly determined in terms of the pipe motion and the dynamics of

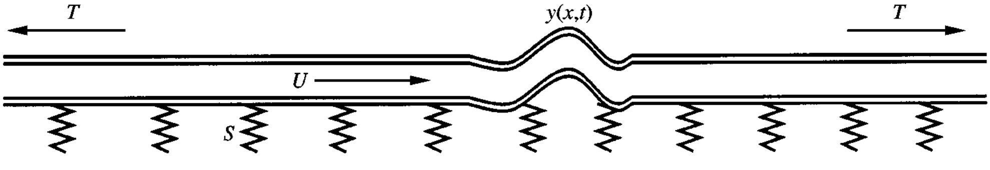

Figure 1. Flexural pipe conveying fluid, with tension and spring foundation.

the coupled system is entirely specified by that of the pipe. In the most general case (Païdoussis & Li 1993), the equation of motion governing the lateral in-plane deflection of the pipe $y(x, t)$ as a function of axial distance x and time t is

$$EI\frac{\partial^4 y}{\partial x^4} + (m + \rho A)\frac{\partial^2 y}{\partial t^2} + (\rho A U^2 - T)\frac{\partial^2 y}{\partial x^2} + 2\rho A U\frac{\partial^2 y}{\partial x \partial t} + Sy = 0, \tag{1}$$

where EI is the flexural rigidity of the pipe, ρA the fluid mass per unit length, U the plug flow velocity, m the mass of pipe per unit length, T a prescribed axial tension, and S the elastic foundation modulus. This relation also describes the in-phase flexural motion of two walls of a channel with plug flow, as will be discussed in the next section. Without flow ($U = 0$), this equation becomes identical to that of a beam with an added mass ρA appearing in the inertia term. With flow ($U \neq 0$), two additional terms are present: a centrifugal term $\rho A U^2(\partial^2 y/\partial x^2)$, which modified the effective tension, and a Coriolis term $2\rho A U(\partial^2 y/\partial x \partial t)$. It should be emphasized that this partial differential equation has a wide range of applicability which is not restricted to inviscid flow (Païdoussis & Li 1993). It is also relevant to the modelling of travelling chains and bands provided one assumes $m = 0$ (Lee & Mote 1997).

The development in space and time of infinitesimal perturbations may be analysed by invoking the notions of absolute and convective instability (Bers 1983). In this framework, the nature of the instability is determined by considering the long-time behaviour of the impulse response $G(x, t)$. The dynamical system is said to be linearly stable if $\lim_{t\to\infty} G(x, t) = 0$ along all rays $x/t =$ constant, and unstable otherwise. Two unstable cases may then be distinguished according to the long-time response at the point of impulse: the instability is said to be convective if $\lim_{t\to\infty} G(0, t) = 0$, the response wavepacket being thus convected away from the source. Conversely, absolute instability refers to the case where $\lim_{t\to\infty} G(0, t) = \infty$, the response then contaminating the entire medium. In practice, such criteria may be expressed in terms of wavenumber k and frequency ω, through the examination of the dispersion equation $D(k, \omega) = 0$ (Bers 1983). The system is stable if $\max_{k \text{ real}} [\mathscr{Im}(\omega(k))] \leq 0$, and unstable otherwise. Consider now the absolute frequency ω_0 such that

$$D(k_0, \omega_0) = 0 \quad \text{and} \quad \frac{\partial D}{\partial k}(k_0, \omega_0) = 0. \tag{2}$$

The absolute or convective nature of the instability is then determined by the sign of its imaginary part $\mathscr{Im}(\omega_0)$. It is said to be absolute if $\mathscr{Im}(\omega_0) > 0$ and convective if $\mathscr{Im}(\omega_0) \leq 0$. In fact, this criterion is not precise enough as it stands and the root (ω_0, k_0) must be associated, as $\mathscr{Im}(\omega)$ decreases from large positive values, with pinching of two branches of the dispersion relation $k^+(\omega)$ and $k^-(\omega)$, that originate respectively in the upper and the lower complex k-plane.

In the next sections, we successively apply these criteria to the various fluid-conveying systems that are represented by equation (1). This is done by first considering models for several limiting cases of the nondimensional parameters, namely the flexural pipe in Section 2, the flexural pipe on an elastic foundation in Section 3, and the tensioned pipe on an elastic foundation, in Section 4. The most general case is then analysed in Section 5.

2. FLEXURAL PIPE

Let us introduce the following nondimensional variables:

$$\tilde{x} = x\sqrt{\frac{\rho}{m}}, \quad \tilde{y} = y\sqrt{\frac{\rho}{m}}, \tilde{t} = t\,\frac{\rho}{m}\sqrt{\frac{EI}{\rho A + m}}, \tag{3}$$

and the nondimensional physical parameters

$$\tilde{U} = U\sqrt{\frac{mA}{EI}}, \quad \beta = \frac{\rho A}{\rho A + m}, \quad \tilde{T} = \frac{mT}{\rho EI}, \quad \tilde{S} = \frac{m^2 S}{\rho^2 EI}, \tag{4}$$

so that equation (1) reads

$$y^{(4)} + \ddot{y} + (\tilde{U}^2 - \tilde{T})y^{(2)} + 2\sqrt{\beta}\,\tilde{U}\dot{y}^{(1)} + \tilde{S}y = 0, \tag{5}$$

where $(\ )^{(n)}$ and $(\dot{\ })$ refer to the space and time derivatives, respectively, and $\tilde{y}$ is denoted by y for simplicity. As a generic case, we consider first the situation where the only mechanical stiffness is due to bending, so that $|\tilde{T}| \ll 1$ and $|\tilde{S}| \ll 1$. From now on in this section, tildes will be omitted from all nondimensional quantities. Equation (5) then becomes

$$y^{(4)} + \ddot{y} + U^2 y^{(2)} + 2\sqrt{\beta}U\dot{y}^{(1)} = 0, \tag{6}$$

a case previously analysed by Kulikovskii & Shikina (1988) and Triantafyllou (1992) and which we shall refer to as the flexural pipe. In should be noted here that our choice of nondimensional parameters differs from that of previous authors. For instance, Gregory & Païdoussis (1966) considered a finite-length pipe, and used the length as reference scale. As in previous studies of infinite media (Crighton & Oswell 1991), the only length scale here is $l = \sqrt{m/\rho}$.

If the pipe displacement is sought in the form $y(x,t) = y_0 \mathrm{e}^{\mathrm{i}(kx-\omega t)}$, the linear dispersion relation is readily obtained as

$$D(k,\omega) = k^4 - U^2k^2 + 2\sqrt{\beta}U\,\omega k - \omega^2 = 0. \tag{7}$$

Before exploring the stability conditions of this generic case, we give below some elements of comparison with the now classical flat-plate problem (Brazier-Smith & Scott 1984; Carpenter & Garrad 1986; Crighton & Oswell 1991). Consider the plug flow of an inviscid incompressible fluid in a plane channel of width e bounded by two parallel elastic plates. If the two plates are restricted to have the same transverse displacement, i.e., if they are subjected to a sinuous mode as opposed to a varicose mode, the equation of motion of each plate may be derived by following the same approach as in Crighton & Oswell (1991) and reads

$$B\frac{\partial^4 y}{\partial x^4} + M\frac{\partial^2 y}{\partial t^2} = \rho\left(\frac{\partial \Phi}{\partial t} + U\frac{\partial \Phi}{\partial x}\right), \tag{8}$$

where B and M are, respectively, the bending stiffness and mass per unit surface of the plate, ρ and U are, respectively, the fluid density and steady velocity, while the velocity potential Φ satisfied

$$\nabla^2\Phi = 0 \tag{9}$$

and the boundary conditions

$$\frac{\partial \Phi}{\partial y}\left(x, -\frac{e}{2}, t\right) = \frac{\partial \Phi}{\partial y}\left(x, \frac{e}{2}, t\right) = \left(\frac{\partial y}{\partial t} + U\frac{\partial y}{\partial x}\right)(x,t). \tag{10}$$

Considering again all dependent variables to be harmonic in t and x, the corresponding dispersion relation is readily obtained as (Walsh 1995)

$$Bk^4 - M\omega^2 - \rho\tanh\left(\frac{ke}{2}\right)\frac{(\omega - Uk)^2}{k} = 0. \tag{11}$$

In the *short-wavelength approximation*, i.e., $ke \gg 1$, we have $\tanh(ke/2) = k/|k|$ and the dispersion relation reduces to

$$Bk^4 - M\omega^2 - \rho\frac{(\omega - Uk)^2}{|k|} = 0. \tag{12}$$

and it is identical to the single flat-plate case (Brazier-Smith & Scott 1984). Similarly, in the *long-wavelength approximation*, $ke \ll 1$, one has $\tanh(ke/2) = ke/2$, so that

$$Bk^4 - M\omega^2 - \rho\frac{e}{2}(\omega - Uk)^2 = 0. \tag{13}$$

If an arbitrary thickness, say h, is then assigned in the out-of-plane direction, we may define for the coupled plates the total bending stiffness $EI = 2hB$, the mass per unit length $m = 2hM$ and the fluid section $A = he$. Upon introducing the nondimensional parameters (3), equation (13) then reduces to the dispersion relation (7) pertaining to the fluid-conveying pipe.

The flexural pipe case and the flat plate case may therefore be understood, respectively, as the long- and short-wave approximation of the more general flexible channel problem. A significant difference between these two limiting cases appears when one considers the flow-induced forces. In the general flexible channel problem as well as its short-wavelength limit (single flat-plate case), the local pressure $p(x,t)$ is obtained by solving the Laplace equation over the whole fluid domain together with the plate boundary conditions. By doing so, the local pressure is influenced by the motion of all points along the plate. In contrast, in the long-wavelength limit, e.g. in the fluid-conveying pipe problem, the local fluid forces only depend on the local displacement: the fluid does not introduce any coupling between various points of the elastic system. This difference is clearly evident when examining the nature of the added mass effects in the simple case of quiescent fluid ($U = 0$). In the short-wavelength approximation (12), fluid forces represented by the last term then remain k-dependent. In the long-wavelength approximation (13), fluid forces represented by the last term are independent of k and may be absorbed as a constant added mass in the inertia term. This feature is well-known in fluid–structure interaction problems (Blevins 1991).

Consider now the development in space and time of bending waves governed by dispersion relation (7), a problem which has been solved by Kulikovskii & Shikina (1988). Let $\Omega = \omega/U^2$ and $K = k/U$, respectively, denote the reduced frequency and the wavenumber. The dispersion relation (7) becomes

$$D(K,\Omega) = K^4 - K^2 + 2\sqrt{\beta}\,\Omega K - \Omega^2 = 0. \tag{14}$$

For real values of the wavenumber, the corresponding frequencies are

$$\Omega = \sqrt{\beta}K \pm K\sqrt{K^2 - (1-\beta)}. \tag{15}$$

When $\beta < 1$, which is the case of fluid-conveying pipes, the system is always unstable in the range of wavenumbers $K^2 < 1 - \beta$. The nature of the instability is given by the absolute frequency Ω_0 defined in equation (2). One finds

$$\Omega_0 = \frac{K_0(1 - 2K_0^2)}{\sqrt{\beta}}, \tag{16}$$

where the absolute wavenumbers satisfies

$$4K_0^4 + K_0^2(3\beta - 4) + (1 - \beta) = 0. \tag{17}$$

The quantity $X = K_0^2$ is seen to be the root of the quadratic polynomial $4X^2 + (3\beta - 4)X + (1 - \beta)$. Let us define the critical mass ratio parameter value

$$\beta_c = \tfrac{8}{9}. \tag{18}$$

If $\beta \geq \beta_c$, the above quadratic polynomial has two positive real roots; K_0 is then real, and so is Ω_0. The instability is therefore convective, but in a marginal sense, as there is no exponential decrease of $G(0, t)$, Ω_0 being only real. If $\beta < \beta_c$, K_0 will have an imaginary part and so will Ω_0. More specifically, equation (17) has four roots two of which being always such that $\mathscr{Im}(\Omega_0) > 0$, thereby indicating absolute instability. In order to confirm this result, it must be checked that pinching of two spatial branches $K^+(\Omega)$ and $K^-(\Omega)$ does take place (Bers 1983). An example of the pinching analysis is presented in Figure 2 for the particular case $\beta = 0{\cdot}5$. The four spatial branches $K(\Omega_R + \mathrm{i}\Omega_I)$ of the dispersion relation (14) are displayed as the imaginary part Ω_I of Ω is gradually lowered. For a given Ω_I, the loci of the spatial branches are obtained by varying the real part Ω_R. Pinching occurs between two acceptable branches and the absolute character of the instability is established. It should be noted that the critical value $\beta_c = \frac{8}{9}$ may also be obtained by exploiting the particular symmetries of the dispersion relation (Crighton & Oswell 1991; Triantafyllou 1992). If (Ω, K) satisfies equation (14), their complex conjugates are also solutions. As the boundary between absolute and convective instability occurs when $\mathscr{Im}(\Omega) = 0$, at transition there must be a triple root of equation (14) which simultaneously satisfies

$$D(K_0, \Omega_0) = \frac{\partial D}{\partial K}(K_0, \Omega_0) = \frac{\partial^2 D}{\partial K^2}(K_0, \Omega_0) = 0. \tag{19}$$

These conditions do give $\beta_c = \frac{8}{9}$, but not the nature of the instability for $\beta < \frac{8}{9}$ and $\beta > \frac{8}{9}$.

3. FLEXURAL PIPE ON AN ELASTIC FOUNDATION

In recent work (Peake 1997), it has been observed that an additional spring stiffness does significantly modify the ranges of convective and absolute instability in the flat-plate problem. Keeping the foundation stiffness $\tilde{S}$ in equation (5), one obtains the nondimensional equation

$$y^{(4)} + \ddot{y} + U^2 y^{(2)} + 2\sqrt{\beta} U \dot{y}^{(1)} + Sy = 0, \tag{20}$$

where the nondimensional stiffness $\tilde{S}$ is written as S for simplicity. It is allowed to be positive or negative in order to provide a simple model for restoring or destabilizing static forces. The corresponding dispersion relation then reads

$$D(k, \omega) = k^4 - U^2 k^2 + 2\sqrt{\beta} U \omega k - \omega^2 + S = 0. \tag{21}$$

The dependence on U may again be simplified by introducing a reduced stiffness $\Sigma = S/U^4$ to yield

$$D(K, \Omega) = K^4 - K^2 + 2\sqrt{\beta}\Omega K - \Omega^2 + \Sigma = 0. \tag{22}$$

According to Roth (1964) and Stein & Trobiner (1970) the system is unstable when

$$\Sigma < \frac{(1 - \beta)^2}{4}. \tag{23}$$

The nature of the instability is again analysed by calculating the roots of equation (2), i.e.,

$$\Omega_0 = \frac{K_0(1 - 2K_0^2)}{\sqrt{\beta}}, \tag{24}$$

where

$$4K_0^6 + K_0^4(3\beta - 4) + K_0^2(1 - \beta) - \Sigma\beta = 0. \tag{25}$$

The absolute frequency Ω_0 is now related to the roots of the third-order polynomial $4X^3 + (3\beta - 4)X^2 + (1 - \beta)X - \Sigma\beta$. Let us define a critical foundation stiffness value

$$\Sigma_c = \frac{\beta_c - \beta}{12\beta}, \tag{26}$$

where $\beta_c = \frac{8}{9}$, as specified in equation (18). If $\Sigma > \Sigma_c$, the three roots are positive real, K_0 is real and so is Ω_0. The instability is then marginally convective as before. It is also necessary that the instability condition (23) be satisfied. Convective instability is then found to exist for $\beta > \frac{2}{3}$ only. If $\Sigma < \Sigma_c$ it may be shown that there always exist two roots Ω_0 with positive imaginary parts, as in the generic case of Section 2. The absolute nature of the instability is established by examining the pinching behaviour of spatial branches as in Figure 2. Again the critical value of Σ_c could be inferred from the triple root criterion, equation (19). The preceding results may also be expressed in terms of the original nondimensional parameters, U and S. Stability is ensured when $U^4 < 4S/(1 - \beta)^2$. For positive foundation stiffness, convective instability is found in the range $4S/(1 - \beta)^2 < U^4 < 12\beta\, S/(\beta_c - \beta)$, if it exists.

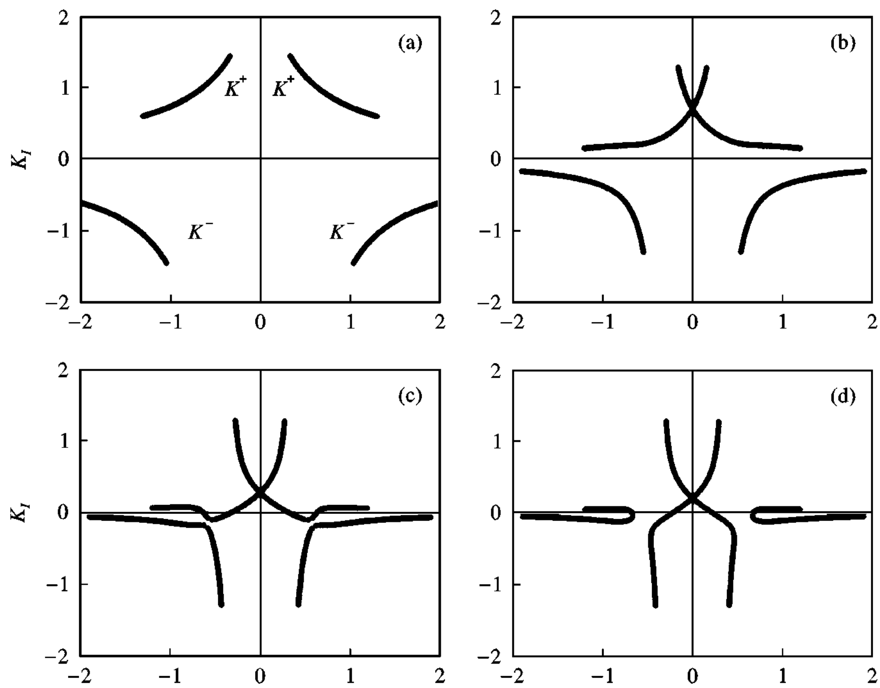

Figure 2. Pinching behaviour of spatial branches in the complex K-plane, $\beta = 0{\cdot}5$, (a) $\Omega_I = 2$; (b)$\Omega_I = 0{\cdot}5$; (c) $\Omega_I = 0{\cdot}2$; (d) $\Omega_I = 0{\cdot}15$. Pinching occurs at $\Omega_I = 0{\cdot}1939$.

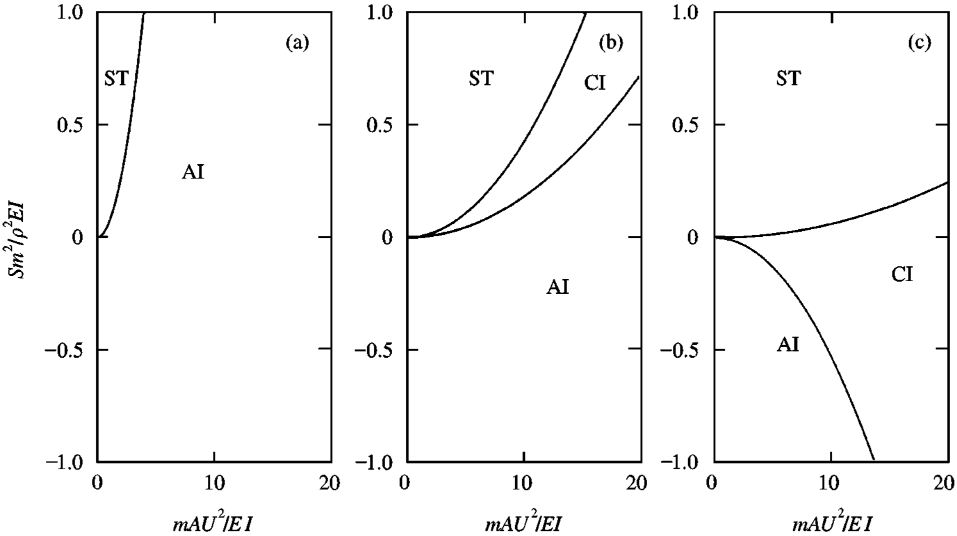

Figure 3. Stability diagram of the flexural pipe with foundation stiffness S, in terms of flow velocity U: stability (ST), absolute instability (AI), convective instability (CI). (a) $\beta = 0{\cdot}5 < \frac{2}{3}$; (b) $\frac{2}{3} < \beta = 0{\cdot}87 < \frac{8}{9}$; (c) $\frac{8}{9} < \beta = 0{\cdot}95 < 1$.

For negative foundation stiffness, it is necessary that $U^4 > 12\beta\, S/(\beta_c - \beta) > 0$ in order to have a convective instability. These various domains are represented in Figure 3, for the three cases $\beta < \frac{2}{3}$, $\frac{2}{3} < \beta < \frac{8}{9}$, and $\frac{8}{9} < \beta < 1$. Depending on the value of β and on the sign of S, a progressive increase in the flow velocity induces quite different transitions: for positive foundation stiffness, $S > 0$, the onset of instability may be either absolute for $\beta < \frac{2}{3}$ or convective for $\beta > \frac{2}{3}$; further transition from convective to absolute instability may appear, but only in the range $\frac{2}{3} < \beta < \frac{8}{9}$. Conversely, for negative foundation stiffness $S < 0$, a transition from absolute to convective instability is found when $\beta > \frac{8}{9}$.

These results are now illustrated by considering the nondimensional Green's function defined by

$$G^{(4)} + \ddot{G} + U^2 G^{(2)} + 2\sqrt{\beta}\, U\, \dot{G}^{(1)} + SG = \delta(x)\delta(t). \tag{27}$$

This corresponds to the response of the fluid-conveying pipe to a short transverse impact of unit momentum. In a Galilean reference frame at the velocity $U\sqrt{\beta}$, the impulse response $\hat{G}(\hat{x}, t) = G(x - U\sqrt{\beta}\, t, t)$ satisfies

$$\hat{G}^{(4)} + \ddot{\hat{G}} + (1 - \beta)U^2 \hat{G}^{(2)} + S\hat{G} = \delta(\hat{x})\,\delta(t). \tag{28}$$

This is the dynamic equation of a beam on an elastic foundation undergoing a static divergence instability, or buckling, under compressive load. When criterion (23) for instability is satisfied the range of unstable wavenumbers is limited by

$$k_{\min}^2 = [(1 - \beta)U^2 - \sqrt{\varDelta}]/2; \quad k_{\max}^2 = [(1 - \beta)U^2 + \sqrt{\varDelta}]/2; \quad \varDelta = (1 - \beta)^2 U^4 - 4S. \tag{29}$$

A straightforward integration over all wavenumbers gives the impulse response

$$G(x, t) = \int_0^\infty f_k(t) \cos[k(x - \sqrt{\beta}\, Ut)]\, \mathrm{d}k, \tag{30}$$

where $f_k(t) = \sinh(\alpha t)/\alpha$ with $\mathrm{a}^2 = k^4 - k^2U^2(1 - \beta) + S$ for unstable wavenumbers, i.e., $k_{\min} < k < k_{\max}$, and $f_k(t) = \sin(\alpha t)/\alpha$ with $\alpha^2 = -[k^4 - k^2U^2(1 - \beta) + S]$ otherwise. This

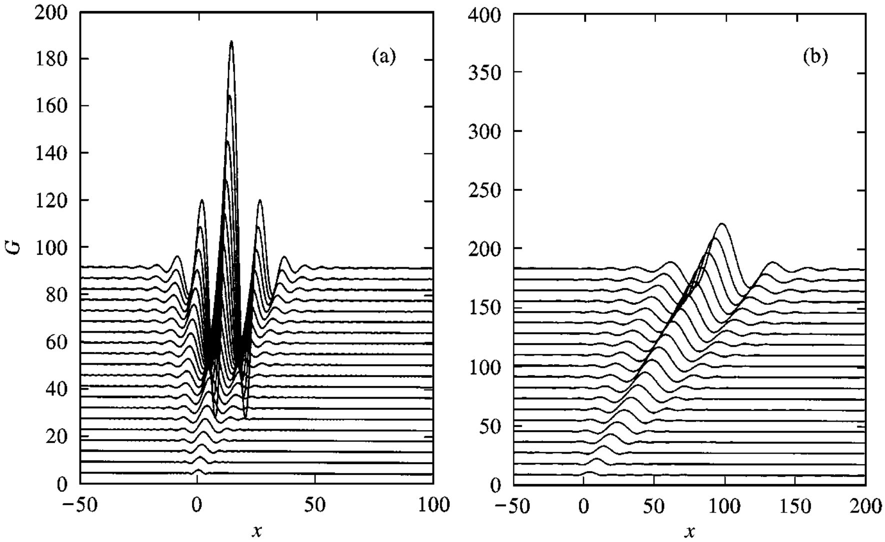

Figure 4. Impulse response of the flexural pipe, $U = 1$, $S = 0$: (a) $\beta = 0{\cdot}5$, absolute instability; (b) $\beta = 0{\cdot}95$, convective instability. The time increment between frames (traces) is $\Delta t = 1$ in (a), and $\Delta t = 5$ in (b).

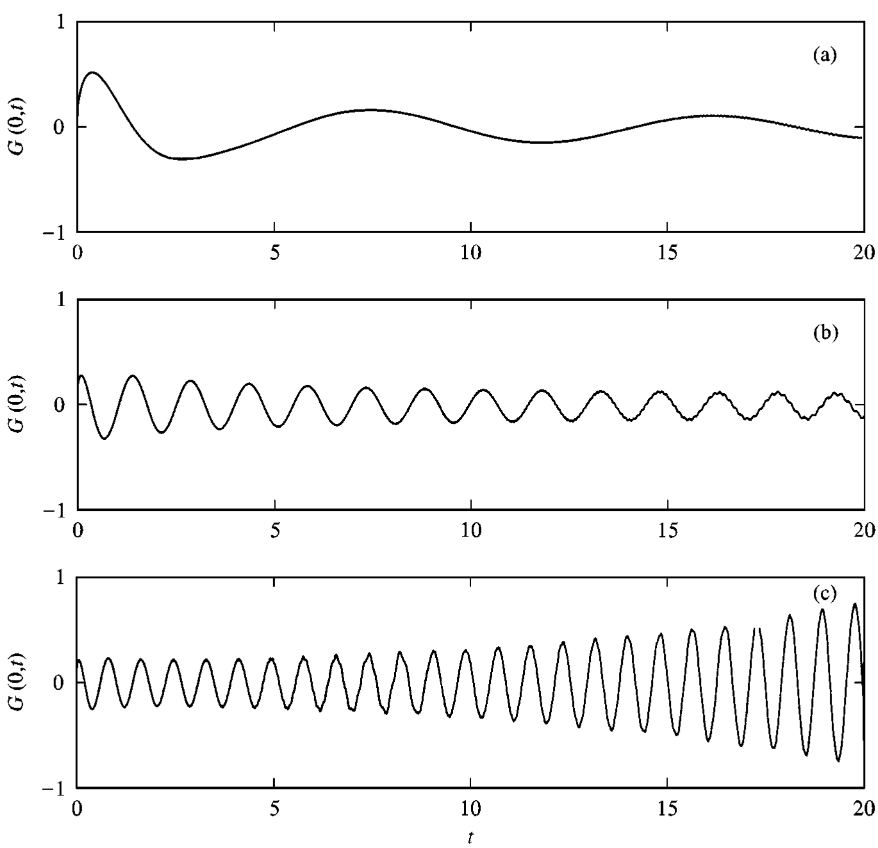

Figure 5. Impulse response at the point of impact for the flexural pipe on an elastic foundation, $\beta = 0{\cdot}85$, $S = 1$. Displacement of the point of impact for increasing flow velocity; (a) $U = 2$, stable case; (b) $U = 3{\cdot}8$, convective instability; (c) $U = 5$, absolute instability.

integral is amenable to a simple numerical integration for any value of the space and time variables. Figure 4 displays the evolution of the pipe displacement with time, in a case of absolute instability $\beta = 0{\cdot}5$, $S = 0$ and a case of convective instability, $\beta = 0{\cdot}95$, $S = 0$. In Figure 5, the response at the point of impact in the case $\beta = 0{\cdot}85$, $S = 1$ illustrates the successive transitions from stability to convective and absolute instability as the flow velocity is progressively increased.

4. PIPE UNDER TENSION

In the limit $\tilde{T} \gg 1$ where tension is large as compared with flexural rigidity, it is convenient to use a different set of nondimensional variables

$$\bar{x} = x\sqrt{\frac{\rho}{m}}, \quad \bar{y} = y\sqrt{\frac{\rho}{m}}, \quad \bar{t} = t\sqrt{\frac{T\beta}{mA}}, \tag{31}$$

and physical parameters

$$\overline{EI} = \frac{1}{\tilde{T}} = \frac{\rho EI}{Tm}, \quad \bar{U} = U\sqrt{\frac{\rho A}{T}}, \quad \beta = \frac{\rho A}{\rho A + m}, \quad \bar{S} = S\frac{m}{\rho T}. \tag{32}$$

Assuming $\overline{EI} \ll 1$, the equation of motion becomes using x, y, t, U, S instead of $\bar{x}$, $\bar{y}$, $\bar{t}$, $\bar{U}$, $\bar{S}$,

$$(U^2 - 1)y'' + \ddot{y} + 2U\sqrt{\beta}\,\dot{y}' + Sy = 0. \tag{33}$$

This lower-order model, which is referred to as the pipe under tension, in analogous to the membrane approximation developed in Carpenter & Garrad (1986) and Kelbert & Sazonov (1996).

When $S = 0$, equation (33) reduces to the wave equation in a moving frame and waves are nondispersive. As for membranes in Carpenter & Garrad (1986), two critical velocities exist corresponding respectively to marginal divergence $U_d = 1$ and wave coalescence $U_c = 1/\sqrt{1-\beta}$. In the more general dispersive case $S \neq 0$ of interest here, it is necessary to consider two different ranges of flow velocities.

When the flow velocity is less than the coalescence velocity, $U < U_c$, a further change of variables $x^* = x/[1 - U^2/U_c^2])^{1/2}$ and $V = U\sqrt{\beta}/[1 - U^2/U_c^2)]^{1/2}$ turns equation (33) into

$$(V^2 - 1)y'' + \ddot{y} + 2V\dot{y}' + Sy = 0, \tag{34}$$

where primes indicate differentiation with respect to x^*. This is the linearized Klein–Gordon equation, which has been extensively studied in the context of marginal stability in inviscid flows. It should be noted that in our case, V can assume all positive values when U is varied from zero to U_c. In the present context, the results of Huerre (1987) for the Klein–Gordon equation translate into the following conclusions: in the range $U < U_c$, the tensioned pipe is stable for $S > 0$, absolutely unstable for $S < 0$ and $0 < U < 1$, and convectively unstable for $S < 0$ and $1 < U < U_c$.

These results may be illustrated by considering the impulse response (Figure 6). In the range $U < U_c$ where the equation reduces to the Klein–Gordon equation, explicit solutions may be derived. When $S > 0$, in the stable range, the response may be adapted from that of a string on a spring foundation (Graff 1975); upon making a Galilean transformation one obtains

$$G(x,t) = \frac{1}{2}\,\mathrm{J}_0\left\{S^{1/2}\left[t^2 - \left(\frac{x - U\sqrt{\beta}t}{1-(1-\beta)U^2}\right)^2\right]^{1/2}\right\}\mathrm{H}\left[t^2 - \left(\frac{x - U\sqrt{\beta}t}{1-(1-\beta)U^2}\right)^2\right], \tag{35}$$

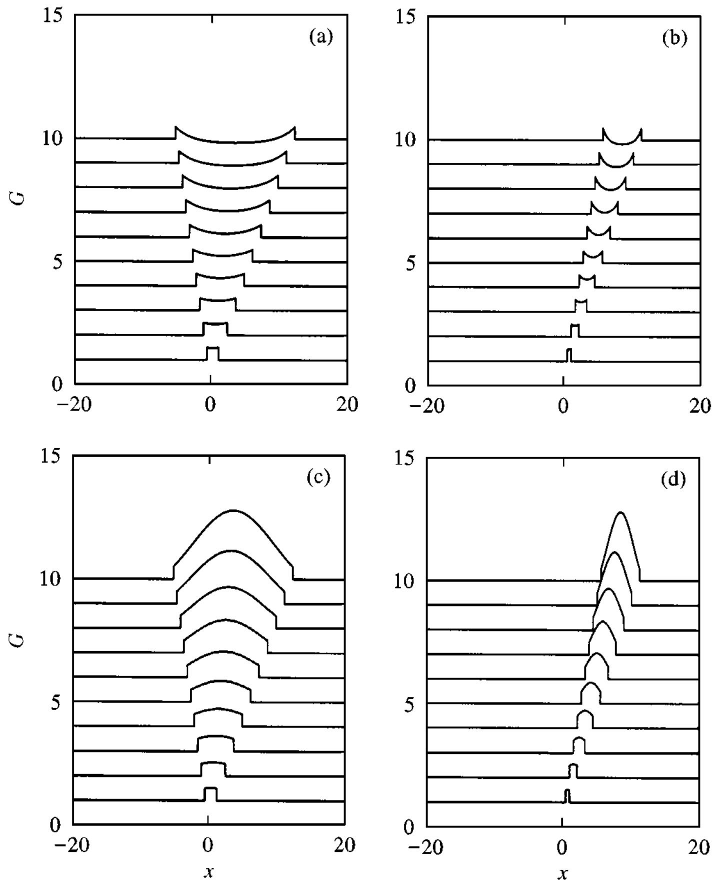

Figure 6. Impulse response of a tensioned pipe, $\beta = 0{\cdot}5$; (a) $U = 0{\cdot}5$, $S = 0{\cdot}1$, stable case; (b) $U = 1{\cdot}2$, $S = 0{\cdot}1$, stable case; (c) $U = 0{\cdot}5$, $S = -0{\cdot}1$, absolutely unstable case; (d) $U = 1{\cdot}2$, $S = -0{\cdot}1$, convectively unstable case. The time increment between frames in $\Delta t = 1$.

where J_0 is the Bessel function and H is the Heaviside step function. Similarly, the unstable case $S < 0$ yields (Huerre 1987)

$$G(x,t) = \frac{1}{2}\,\mathrm{I}_0\left\{(-S)^{1/2}\left[t^2 - \left(\frac{x - U\sqrt{\beta}t}{1-(1-\beta)U^2}\right)^2\right]^{1/2}\right\}\mathrm{H}\left[t^2 - \left(\frac{x - U\sqrt{\beta}t}{1-(1-\beta)U^2}\right)^2\right], \quad (36)$$

where I_0 is the modified Bessel function.

A completely new situation arises after coalescence, when $U > U_c$, where equation (33) is not reducible to the Klein–Gordon equation. It is then necessary to use a different transformation of variables $x^* = x/[(U^2/U_c^2] - 1)^{1/2}$ and $V = U\sqrt{\beta}/[(U^2/U_c^2) - 1]^{1/2}$ which now yields

$$(V^2 + 1)y'' + \ddot{y} + 2V\dot{y}' + Sy = 0. \quad (37)$$

The corresponding dispersion relation reads

$$-(V^2 + 1)k^2 - \omega^2 + 2V\omega k + S = 0, \quad (38)$$

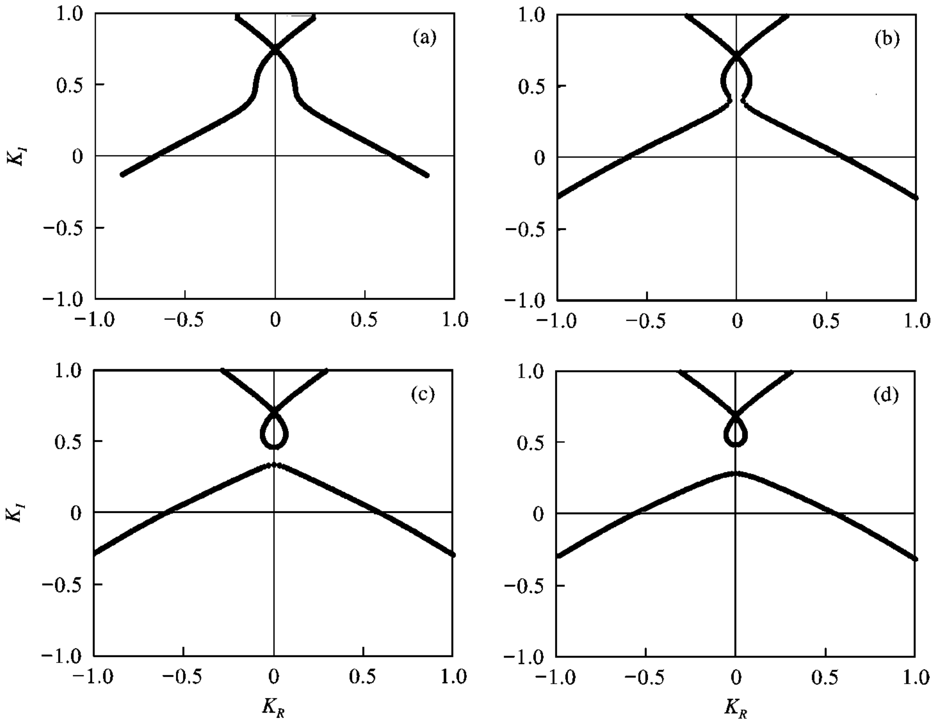

Figure 7. Pinching behaviour for the pipe under tension, $\beta = 0{\cdot}5$, $U = 3$, $S = -1$: (a) $\Omega_I = 1{\cdot}6$; (b) $\Omega_I = 1{\cdot}52$; (c) $\Omega_I = 1{\cdot}49$; (d) $\Omega_I = 1{\cdot}45$. Pinching occurs at $\Omega_I = 4/\sqrt{7} = 1{\cdot}512$ but it does not involve k^+ and k^- branches emanating from distinct halves of the complex k-plane.

so that

$$\omega = kV \pm \sqrt{S - k^2}. \tag{39}$$

The system is therefore unstable for any value of S, but here for high wavenumbers as opposed to the case of a flexural pipe. Moreover, the temporal growth rate given by equation (39) increases indefinitely with wavenumber. As a result of this pathological behavior, causality cannot be enforced. This is also apparent in the pinching analysis of the k-branches as seen in Figure 7. In practice, one should note that in any physical situation the present model is not applicable when the wavelength becomes comparable to the pipe thickness. Furthermore, flexural stiffness does play an increasing role at short wavelengths, when compared with stiffness due to tension. It is therefore reasonable to consider that a characteristic length exists in practice that bounds the range of unstable wavelengths. To further analyse the nature of the instability that arises beyond coalescence, we consider in the next section the simultaneous effect of tension and flexural rigidity in order to introduce a cut-off wavenumber.

5. GENERAL CASE

When all stiffness terms are present, namely flexural rigidity, tension and spring foundation, the nondimensional equation of motion is equation (5). A straightforward analysis of the imaginary part of the frequency for real wavenumbers yields that the pipe is only stable when (Roth 1964)

$$\tilde{S} > 0 \quad \text{and} \quad \tilde{U}^2 < \frac{2\sqrt{\tilde{S}} + \tilde{T}}{1-\beta}. \tag{40}$$

In the limit $\tilde{T} = 0$, the stability criterion of Section 3 is recovered. Conversely, the pure tension case may be obtained when equation (40) is written in terms of nondimensional variables based on tension, as in Section 4. The stability criterion reads

$$\bar{S} > 0 \quad \text{and} \quad \bar{U}^2 < \frac{2\sqrt{\bar{S}\,\overline{EI}} + 1}{1-\beta}. \tag{41}$$

With a vanishing flexural rigidity $\overline{EI} = 0$, equation (41) reduces to the coalescence criterion.

In order to clarify the noncausal situation that arose in the preceding section, consider now the nature of the instability in the range of velocities $\tilde{U}^2 > \tilde{T}/(1-\beta)$. Let us define a modified velocity $\tilde{V}^2 = \tilde{U}^2 - \tilde{T}$ and mass ratio $\gamma = \beta\tilde{U}^2/(\tilde{U}^2 - \tilde{T})$. Equation (5) then reads

$$y^{(4)} + \ddot{y} + \tilde{V}^2 y^{(2)} + 2\sqrt{\gamma}\,\tilde{V}\,\dot{y}' + \tilde{S}y = 0, \tag{42}$$

which is identical to equation (20) of Section 3 when tension effects were neglected. Note that the modified mass ratio γ varies between β and 1 as $\tilde{U}$ varies in the range under consideration, so that the results of Section 3 are applicable. It is found that a transition between convective and absolute instability occurs at values of $\tilde{U}$ defined by

$$[\tilde{U}^2 - \tilde{T}]^2\,[\tilde{U}^2(\beta_c - \beta) - \beta_c\tilde{T}] - 12\beta\tilde{S}\tilde{U}^2 = 0. \tag{43}$$

This criterion may also be expressed in terms of non-dimensional variables pertaining to the tensioned case:

$$[\bar{U}^2 - 1]^2[\bar{U}^2(\beta_c - \beta) - \beta_c] - 12\beta\bar{S}\,\overline{EI}\,\bar{U}^2 = 0. \tag{44}$$

The particular solution of Triantafyllou (1992) for the tensioned pipe without spring foundation is readily obtained for $\tilde{S} = 0$.

Figures 8 and 9 display the evolution of these domains, as defined by equations (41) and (44). Depending on the value of β, two cases need to be considered. When $\beta < \beta_c$, Figure 8(a, b), two distinct domains of convective and absolute instability persist as the non-dimensional flexural rigidity $\overline{EI}$ is decreased. It may be inferred that the limiting case of vanishing flexural rigidity $\overline{EI} = 0$ gives rise to the stability diagram depicted in Figure 8(c), which precisely coincides with the tensioned pipe. When $\overline{EI} = 0$, a transition from convective to absolute instability exists at $\bar{U}^2 = \beta_c/(\beta_c - \beta)$. It may be shown that the corresponding nondimensional absolute frequency based on tension scales as

$$\bar{\omega}_0 = \frac{1}{\sqrt{\overline{EI}}}\,(\bar{U}^2 - 1)\,\Omega_0, \tag{45}$$

so that the robustness of the pinching is ensured in the limit of vanishing flexural rigidity $\overline{EI} \to 0$. Conversely, when $\beta > \beta_c$, Figure 9(a, b), the region of absolute instability moves off to unattainable negative values of $\bar{S}$ as $\overline{EI}$ is lowered. By going to the limit $\overline{EI} = 0$, Figure 9(c), convective instability therefore prevails for the tensioned pipe beyond coalescence. By exploiting the results of Section 4 pertaining to pre-coalescence values of

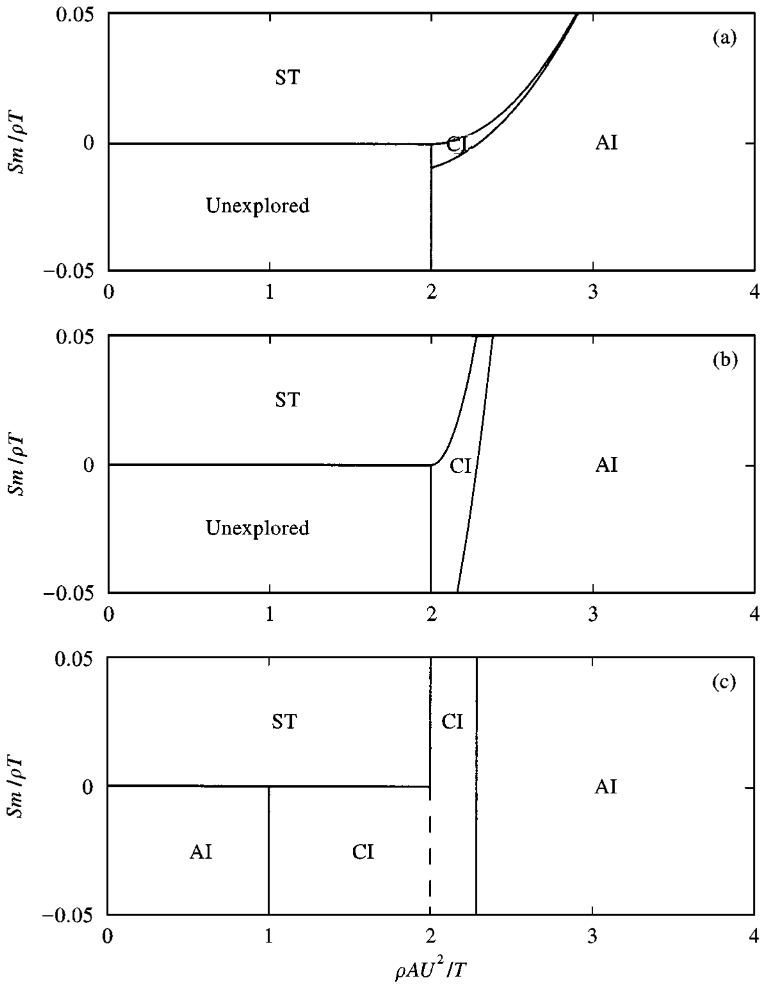

Figure 8. Stability diagram in the $\bar{U}^2$ versus $\bar{S}$ plane for the general case with $\beta = 0{\cdot}5 < \beta_c$. Stability (ST), absolute instability (AI), convective instability (CI). (a) $\overline{EI} = 1$; (b) $\overline{EI} = 0{\cdot}1$; (c) $\overline{EI} = 0$, tensioned pipe.

velocities, $\bar{U} < \bar{U}_c$, the tensioned pipe stability diagram may be completed as sketched in Figures 8(c) and 9(c).

6. CONCLUDING REMARKS

In this paper, we have systematically investigated the nature of the various instabilities that may arise in a fluid-conveying pipe on an elastic foundation, thus extending the results of Kulikovskii & Shikina (1988) for the flexural pipe and Triantafyllou (1992) for the flexural pipe with tension. For the simple models that have been considered here, closed-form solutions have been derived for the boundaries between convective and absolute instability in control parameter space. Furthermore, the impulse response has been expressed in a simple integral form that is amenable to numerical integration.

We have analysed the various effects of the physical parameters, namely the tension, the flexural rigidity, the fluid velocity, the mass ratio and the foundation stiffness. By considering the limit models of flexural pipes and tensioned pipes, as well as the general case, we

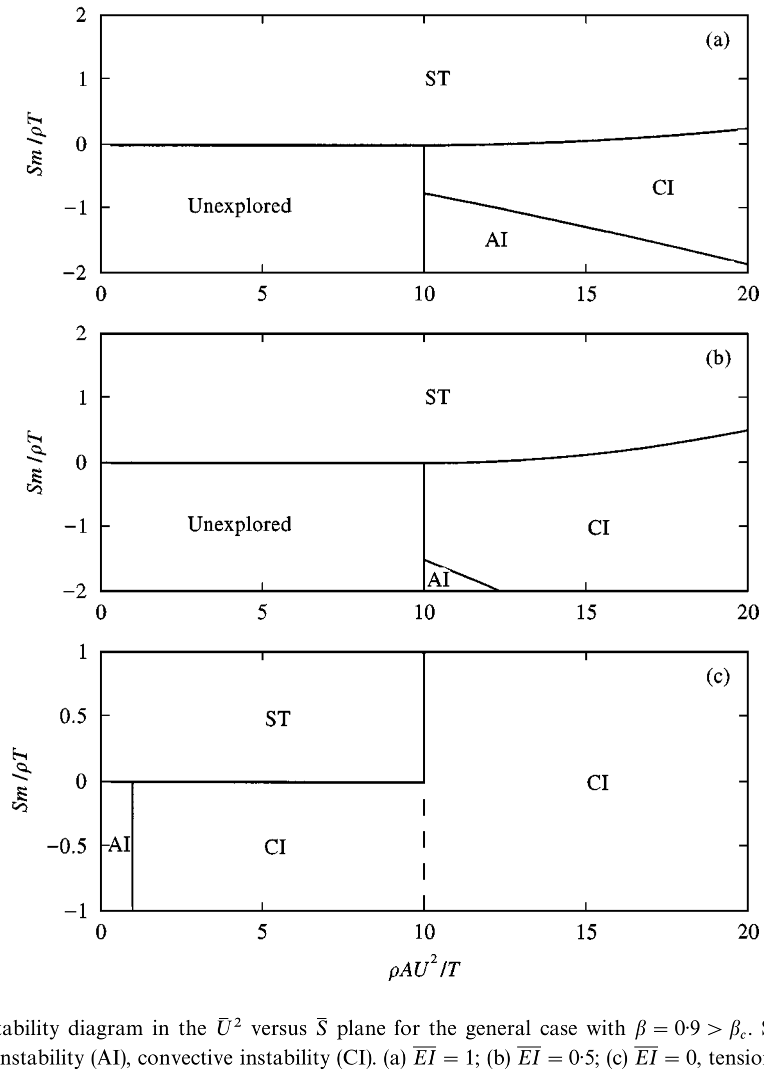

Figure 9. Stability diagram in the $\bar{U}^2$ versus $\bar{S}$ plane for the general case with $\beta = 0{\cdot}9 > \beta_c$. Stability (ST), absolute instability (AI), convective instability (CI). (a) $\overline{EI} = 1$; (b) $\overline{EI} = 0{\cdot}5$; (c) $\overline{EI} = 0$, tensioned pipe.

have shown that the ratio between the flexural rigidity and that induced by tension plays a crucial role in the dynamics of the system. Absolute instability has been shown to widely prevail in the case of a flexural pipe with a spring foundation. Conversely, convective instability is much more likely to be found in a tensioned pipe. As to this difference, it should be recalled that the flexural model yields waves of infinite phase velocities, which is not the case for the tensioned pipe (Graff 1975). In this sense the possibility exists in flexural pipes that the upstream going unstable waves of high velocity overcome the global advection of the wavepacket, thereby bringing about an absolute instability. In the tensioned pipe, the phase velocity is bounded and a sufficiently large convection velocity will prevent absolute instability. This has been shown in earlier work on the Klein–Gordon equation (Huerre 1987) of which the tensioned pipe problem is a generalization.

When the fluid velocity is progressively increased, different types of transitions occur depending on the range of the other parameters. Denoting stability, convective and absolute instability by ST, CI and AI respectively, one observes the following variety of scenarios:

ST-AI, ST-CI-AI, ST-CI, AI-CI and even AI-CI-AI. This complex influence of the fluid velocity may be understood by realizing that it plays a double role in the dynamics of the system: on the one hand it advects the perturbations, thereby favouring convective instability, and on the other it increases the instability growth rate.

The effect of the mass ratio between the fluid and the pipe represented by β appears in the dimensional convection velocity $U\beta$ of the centre of the wavepacket. The impulse response travels at a velocity lower than the fluid velocity by a factor equal to the mass ratio β (Roth 1964). Convective instabilities are therefore most likely to arise at high mass ratios. This is precisely what is found in all the cases we have considered. In practice, values of β are typically of the order of 0·5 because of the pipe thickness required for pressure confinement. Yet, the particular case $\beta = 1$ is also of some interest as it represents the case of travelling chains and bands or chain-saw blades, where the fluid/solid media of the present work are replaced by a single moving elastic medium (Lee & Mote 1997). In this limit, any positive elastic foundation stabilizes the flexural system, and negative values allow transition between absolute and convective instability as the travelling velocity is increased. For tensioned media, the situation is then totally reducible to the Klein–Gordon equation.

The foundation stiffness S, considered here positive or negative, has a strong influence on both the stability limits and the nature of the instability, in a manner similar to that found in Peake (1997).

In the present analysis, the effect of damping has not been considered. The stability threshold for the general case, equation (40), is known to be significantly modified as soon as dissipation is included in the model (Roth 1964; Païdoussis 1998). This is related to the destabilizing effect of damping. The limits between domains of convective and absolute instabilities should then also be reanalysed, and some substantial modifications may be expected as for other systems (Carpenter & Garrad 1986; Peake 1997). More generally, the concept of negative-energy waves would be helpful to give some physical understanding of the mechanisms involved (Triantafyllou 1992; Païdoussis 1998).

All the solutions presented here have been derived in the frame of a linear analysis and with a plug-flow approximation. These are known to yield results qualitatively applicable to a large range of geometrical parameters, as discussed in Païdoussis (1998).

We have indicated that the flexural pipe model bears some similarity with the flexible flat plate case considered by Brazier-Smith & Scott (1984). These authors did find a transition from convective to absolute instability, but it has been demonstrated by Peake (1997) that this occurs only in unrealistic ranges of physical parameters: in contrast to the flexural pipe, convective instability actually prevails for the flexible flat plate. Conversely, when the flexible plate is replaced by a tensioned flat plate, i.e., a membrane, it has been shown by Kelbert & Sazonov (1996) that convective instability takes place only in a very small range of flow velocities and that absolute instability therefore prevails. The tensioned pipe problem analysed in the present work also bears some similarity to this membrane case. We have shown in Section 5 that the range for convective instability that arises for pipes under tension is strongly dependent on the mass ratio β. However, as soon as the mass ratio exceeds the small value of $\beta = 0{\cdot}25$, the flow velocity range for convective instability becomes larger than in the membrane case. It may therefore legitimately be concluded that convective instability dominates for the tensioned pipe, whereas absolute instability dominates for the membrane. This conclusion is reversed when comparing the flexural pipe with the flexural plate. Such differences between models assuming semi-infinite or confined fluid domains have not been explained. We believe that this might be related to the local nature of fluid forces associated with fluid-conveying pipes, as discussed in Section 1. Yet, it appears that the results obtained with models of fluid-conveying pipes are much simpler and probably less pathological than those derived from the flat-plate or membrane problems.

The various types of instabilities of modes arising in pipes of *finite length* have in many cases been satisfactorily interpreted in terms of the exchange of energy between the fluid and the pipe that arise at the ends (Païdoussis 1987). It is hoped that, as in the field of hydrodynamic stability (Huerre & Monkewitz 1990), an understanding of these global instabilities might be gained from the knowledge of the absolute/convective nature of the instability within the bulk of the medium. More generally, Païdoussis & Li (1993) have demonstrated that the fluid-conveying pipe constitutes a "model dynamical problem" for one-dimensional systems of *finite* extent. The present results as well as recent work on wave energetics (Triantafyllou 1992) or weakly nonuniform media (Kulikovskii 1993) have further indicated that the fluid-conveying pipe may also serve as a convenient archetype in the study of instabilities in *infinitely extended* one-dimensional systems.

ACKNOWLEDGEMENTS

The authors wish to acknowledge fruitful discussions with Patrick Huerre (LadHyX, Ecole Polytechnique) and Nigel Peake (DAMTP, University of Cambridge).

References

Benjamin, T. 1963 The threefold classification of unstable disturbances in flexible surfaces bounding inviscid flow. *Journal of Fluid Mechanics* **16,** 436–450.

Bers, A. 1983 Space-time evolution of plasma instabilities-absolute and convective. In *Handbook of Plasma Physics* (eds M. Rosenbluth & R. Sagdeev), Volume 1, pp. 451–517, Amsterdam: North-Holland.

Blevins, R. D. 1991 *Flow-Induced Vibration*, 2nd edition. New York: Van Nostrand Reinhold.

Bourrières F. 1939 Sur un phénomène d'oscillation auto-entretenue en mécanique des fluides réels. *Publications Scientifiques et Techniques du Ministere de l' Air*, No. 147.

Brazier-Smith, P. & Scott, J. 1984 Stability of fluid flow in the presence of a complaint surface. *Wave Motion* **6,** 574–560.

Carpenter, P. & Garrad, A. D. 1986 The hydrodynamic stability over Kramer type compliant surfaces. Part 2. Flow-induced surface instabilities. *Journal of Fluid Mechanics* **170,** 199–232.

Crighton, D. & Oswell, J. E. 1991 Fluid loading with mean flow. I. Response of an elastic plate to localized excitation. *Philosophical Transactions of the Royal Society of London* A **335,** 557–592.

Graff, K. 1975 *Wave Motion in Elastic Solids*. Ohio State University Press.

Gregory, R. W. & Païdoussis, M. P. 1966 Unstable oscillation of tubular cantilevers conveying fluids. I. Theory, *Proceedings of the Royal Society of London* A **293,** 512–527.

Huerre, P. 1987 Spatio-temporal instabilities in closed and open flows. In *Instabilities and Non-Equilibrium Structures* (eds E. Tirapegui & D. Villaroel), pp. 141–177. Dordrecht: Reidel.

Huerre, P. & Monkewitz, P. 1990 Local and global instabilities in spatially developing flows. *Annual Review of Fluid Mechanics* **22,** 473–537.

Kelbert, M. & Sazonov, I. 1996 *Pulses and Other Wave Processes in fluids*. Modern Approaches in Geophysics. Dordrecht: Kluwer Academic.

Kulikovskii, A. 1993 On the stability of weakly non-uniform flows in extended regions. *Journal of Applied Mathematics and Mechanics* **57,** 851–856.

Kulikovskii, A. G. & Shikina, I. S. 1988 On the bending oscillation of a long tube filled with moving fluid. *Izvestia Akademii Nauk Arminskoi SSR* **41,** 31–39.

Landahl, M. 1962 On the stability of a laminar incompressible boundary layer over a flexible surface. *Journal of Fluid Mechanics* **13,** 609–632.

Lee, S. & Mote, Jr, C. 1997 A generalized treatment of the energetics of translating continua Part I. Strings and second order tensioned pipes. *Journal of Sound and Vibration* **204,** 717–734.

Lucey, A. & Carpenter, P. 1992 A numerical simulation of the interaction of a compliant wall and an inviscid flow. *Journal of Fluid Mechanics* **234,** 121–146.

PAÏDOUSSIS, M. P. 1987 Flow-induced instabilities of cylindrical structures. *Applied Mechanics Review* **40,** 163–175.

PAÏDOUSSIS, M. P. & LI, G. 1993 Pipes conveying fluid: a model dynamical problem. *Journal of Fluids and Structures* **7,** 137–204.

PAÏDOUSSIS, M. P. 1998 *Fluid–structure Interactions: Slender Structures and Axial Flow*. Volume 1. London: Academic Press.

PEAKE, N. 1997 On the behaviour of a fluid-loaded cylindrical shell with mean flow. *Journal of Fluid Mechanics* **338,** 387–410.

ROTH, W. 1964 Instabilität durchströmter Rohre. *Ingenieur Archiv* **33,** 236–263.

STEIN, R. A. & TOBRINER, M. 1970 Vibration of pipes containing flowing fluids. *Journal of Applied Mechanics* **37,** 906–916.

TRIANTAFYLLOU, G. S. 1992 Physical condition for absolute instability in inviscid hydroelastic coupling. *Physics of Fluids* A **4,** 544–552.

WALSH, C. 1995 Flutter in one-dimensional collapsible tubes. *Journal of Fluids and Structures* **9,** 393–408.